Intriguing influence of -COOH-driven intermolecular aggregation and acid-base interactions with DMF on the second order NLO response of 5,15 push-pull diaryl Zn^{II} porphyrinates

Alessio Orbelli Biroli[§], Francesca Tessore[†], Stefania Righetto[†], Alessandra Forni*[§], Alceo Macchioni[‡], Luca Rocchigiani[‡], Maddalena Pizzotti[†], Gabriele Di Carlo[†].*

[§] Istituto di Scienze e Tecnologie Molecolari del CNR (CNR-ISTM), SmartMatLab Centre, via C. Golgi, 19 – 20133 Milano (Italy).

[†] Dipartimento di Chimica, Università degli Studi di Milano, Unità di Ricerca dell'INSTM, via C. Golgi, 19 – 20133 Milano (Italy)

[‡] Dipartimento di Chimica, Biologia e Biotecnologie and CIRCC, Università degli Studi di Perugia, via Elce di Sotto, 8 – 06123 Perugia (Italy)

KEYWORDS: Zn^{II} porphyrinates; push-pull; NLO properties; DFT calculations; aggregation

Abstract A series of 5,15 *meso* push-pull diaryl ZnII porphyrinates, carrying one or two –COOH or $–COOCH_3$ acceptor groups and a $–OCH_3$ or a $–N(CH_3)_2$ donor group show in both DMF and $CHCl_3$ solution a negative and solvent dependent second order NLO response measured by the EFISH technique, differently from the structurally related Zn^{II} porphyrinate carrying a $–N(CH_3)_2$ donor and a $–NO_2$ acceptor group, where a still solvent dependent, but positive EFISH second order response was previously reported. Moreover, when a $–N(CH_3)_2$ donor group and a –COOH acceptor group are part of a sterically hindered 2,12 push-pull β-pyrrolic substituted tetraaryl ZnII porphyrinate, the EFISH response is positive and solvent independent. In order to rationalize these rather intriguing series of observations, EFISH measurements have been integrated by electronic absorption and infrared spectroscopic investigations and by DFT and CP-DFT theoretical and ^1H PGSE NMR investigations, which prompt that the significant concentration effects and the strong influence of the solvent nature on the NLO response are originated by a complex whole of different aggregation processes induced by the –COOH group.

Introduction

In the last two decades a large effort was devoted to the definition of the main structural features of organic or organometallic molecular chromophores to reach a significant second order nonlinear optical (NLO) response.

According to the so-called "two-level" model developed in 1977 by Oudar,[1,2] the quadratic hyperpolarizability (β) of a molecule originates from the mobility of polarizable electrons under a strong electric field (such as the one associated to laser radiation) and depends on electronic charge-transfer (CT) transitions. Assuming that the second order NLO response is dominated by one major CT process, β_{zzz} can be defined according to equation 1:

$$\beta_{zzz} = \frac{3}{2h^2c^2}\frac{\nu_{eg}^2 r_{eg}^2 \Delta\mu_{eg}}{(\nu_{eg}^2-\upsilon_L^2)(\nu_{eg}^2-4\upsilon_L^2)} \quad (1)$$

where z is the axis of the direction of the CT, ν_{eg} (cm^{-1}) the frequency of the CT transition, r_{eg} the transition dipole moment, $\Delta\mu_{eg}$ the difference between the excited and the ground state dipole moment, and ν_L the frequency of the incident radiation.

Noncentrosymmetric molecules with CT transition at relatively low energy with large $\Delta\mu_{eg}$ and r_{eg} (the so-called "push-pull" structures, in which an electron-donor and an electron-acceptor group are linked through a π-conjugated polarizable spacer) are therefore those fulfilling the electronic requirements for a high β value.

Another essential issue is the determination of the inherent molecular NLO response in solution, devoid of possible effects associated with solute/solute and/or solute/solvent intermolecular interactions, which could bias the NLO response.[3]

Among the many examples of NLO molecular chromophores reported in the literature,[4,5] push-pull diarylmetalporphyrinates, carrying in 5,15 *meso* positions a donor and an acceptor aromatic ring connected by a triple bond to the porphyrinic core, firstly reported by Therien and co-workers[6,7,8] and subsequently deepened by some of us,[9,10] are characterized by a significant quadratic hyperpolarizability[6-10] and two-photon absorption.[11,12] As first reported by some of us through an *ab initio* TD-DFT investigation,[13] the second order NLO response is mainly due to the directional HOMO-LUMO CT transition along the push-pull system, which gives rise to a quite strong Q absorption band between 600 and 700 nm.

It was reported that the peculiarity of the Zn^{II} complexes of these push-pull porphyrinic NLO chromophores, carrying a $–NO_2$ acceptor group, is a strong solvent effect on the second order NLO response, which appears positive and higher when measured in a solvent of low polarity and acidic properties like $CHCl_3$ than in a solvent of higher polarity and basic properties like

DMF.[10] Moreover, the NLO response is greatly affected by the nature of the central metal atom of the porphyrinic ring, decreasing significantly in $CHCl_3$ solution when the Zn atom is replaced by the Ni atom.[10]

In particular, in $CHCl_3$ solution the Zn^{II} chromophore exists, at least in part, as a head-to-head J-aggregate (J_{hh}), due to the axial interaction of the acid Zn^{II} centre of one molecule with the dimethylamino donor group of the push-pull system of another molecule. Such J-aggregation is the origin of a large increase of the second order NLO response. On the contrary in DMF, where such intermolecular acid-base aggregation is hindered owing to the preferential axial coordination of the basic solvent to the Zn^{II} ion, the quadratic hyperpolarizability becomes about one half of the value recorded in $CHCl_3$ solution, at the same concentration.[10,13]

More recently, this kind of 5,15 push-pull diaryl Zn^{II} porphyrinates were largely investigated as interesting sensitizers for Porphyrin-Sensitized Solar Cells (PSSCs).[14] Our group, also involved in this research area, synthesized a series of 5,15 push-pull diaryl Zn^{II} porphyrinates, structurally analogous to those previously investigated for their second order NLO properties,[6-10] but carrying, instead of an acceptor $–NO_2$ group, one[15] or two[16] -COOH groups, necessary to assure the anchoring of the porphyrinic sensitizer to the TiO_2 semiconductor surface of the solar cell.

Therefore we extended our investigation to the second order NLO response, measured by the Electric Field Induced Second Harmonic generation (EFISH) technique,[17-19] of these new push-pull porphyrinic chromophores, for which the presence of one or two -COOH or $–COOCH_3$ groups could introduce additional aggregation processes and more significant acid-base interactions with a basic solvent like DMF.

In fact, DMF is able to interact by hydrogen-bond with the -COOH group.[20] Moreover, it is well known that benzoic acid and generally carboxylic acids, particularly in non-polar solvents like $CHCl_3$, may dimerize by hydrogen bond to form a cyclic 1:1 dimeric species.[21]

The structures of all the investigated 5,15 push-pull diaryl Zn^{II} porphyrinates are depicted in Chart 1. Chromophores **1-4** carry one (**1-3**) or two (**4**) –COOH acceptor groups, and, with the only exception of **1**, the strong $–N(CH_3)_2$ electron donor group. For comparative purposes we also synthesized the corresponding esters **2bis** and **5**, the 5,15 push-pull Zn^{II} porphyrinate **6** analogous to **1** but with a $–NO_2$ instead of a -COOH acceptor group and also the structurally different and more sterically hindered β-substituted 2,12 push-pull tetraaryl Zn^{II} porphyrinate **7**.

Hereafter we report the results of a comprehensive investigation aimed at rationalizing the intriguing role of the intermolecular interactions and solvation effects which may control the second order NLO response of chromophores **1-7** in $CHCl_3$ and DMF solution. The investigation was carried out by DFT and CP-DFT calculations, electronic absorption and infrared spectroscopy (when necessary), and EFISH measurements in $CHCl_3$ and DMF solution. Finally a ^1H Pulsed Gradient Spin Echo (PGSE) NMR investigation[22-25] of the structurally different chromophores **2** and **5** in $CDCl_3$ and DMF-d_7 solution was carried out with the aim of evaluating the entity of their intermolecular aggregation in solution and therefore the role of the -COOH group.

Chart 1 Investigated porphyrinic chromophores

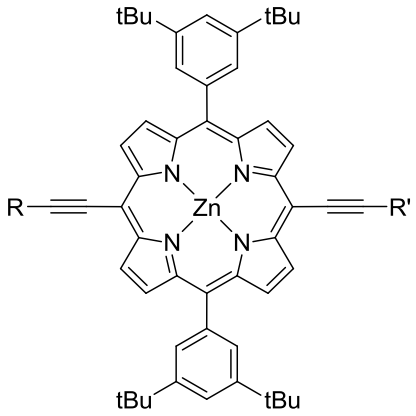

5,15 meso diaryl Zn^{II} porphyrinates

compound	R	R'
1	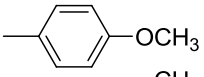	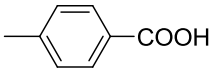
2	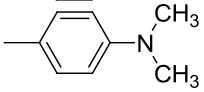	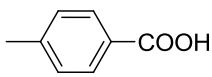
2bis	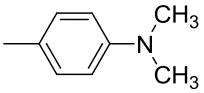	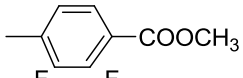
3	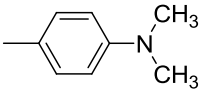	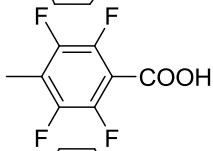
4	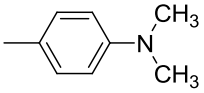	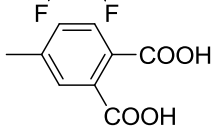
5	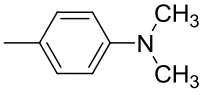	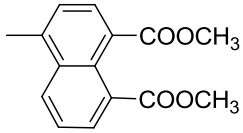
6	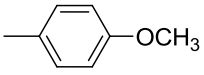	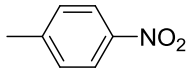

2,12 b-pyrrolic tetraaryl Zn^{II} porphyrinate

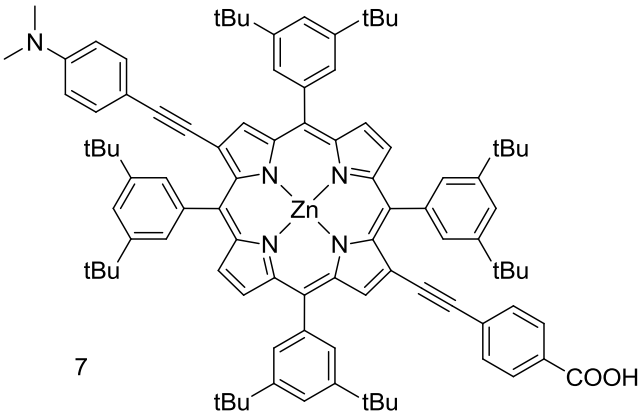

7

Experimental section

General remarks

All the reagents and the solvents used in the syntheses were purchased from Sigma Aldrich and used as received, except NEt_3 and NEt_2NH (freshly distilled over KOH) and THF (freshly distilled from Na/benzophenone under dinitrogen). 4-Bromo-1,8-naphthalic anhydride was purchased from ABCR. Silica gel for gravimetric chromatography (Geduran Si 60, 63-200 μm) and for flash chromatography (Kieselgel 60, 0.040-0.063 mm) were purchased from Merck. [5,15-diiodo-10,20-bis(3,5-di-tert-butylphenyl)porphyrinate]Zn^{II} and chromophores **1-3**,[15] **4** and **7**,[16] and **6**[26] were prepared as reported in the literature. The details on the synthesis of **2bis** and **5** and of their precursors, including their ^{1}H-NMR spectra, are reported in the SI.

^{1}H-NMR spectra were recorded on a Bruker Avance DRX-400 in pure $CDCl_3$, in $CDCl_3$ with addition of pyridine-d_5 or in THF-d_8 (Cambridge Isotope Laboratories, Inc.). Mass spectra were obtained with a Bruker-Daltonics ICR-FTMS APEX II with an electrospray ionization source (SI) or on a VG Autospec M246 magnetic mass spectrometer with a LSIMS ionic source. Electronic absorption spectra were recorded in $CHCl_3$ and DMF solutions at room temperature on a Shimadzu UV 3600 spectrophotometer. IR spectra were recorded in $CHCl_3$ solution on a Jasco FT/IR-410 spectrophotometer.

EFISH measurements

The second order NLO responses of chromophores **1-7** were measured by the EFISH technique,[17-19] using a prototype apparatus made by SOPRA (France), and working with a 1907 nm incident wavelength. For each chromophore measurements were performed on freshly prepared solutions in DMF at 10^{-3} M concentration and in $CHCl_3$ at $5x10^{-4}$ M concentration, due to the lower solubility in this latter solvent. For compound **6** in $CHCl_3$ the measure was

performed at $5x10^{-5}$ M concentration. For chromophores **1**, **2**, **2 bis**, **3** and **5** in DMF (and for chromophore **2** in $CHCl_3$), the second order response of $5x10^{-4}$ M and 10^{-4} M solutions was also investigated.

The 1907 nm laser incident wavelength was chosen because its second harmonic (at 953 nm) is far enough from the absorption bands of the chromophores in $CHCl_3$ (λ_{max} of the B band in the range 440-460 nm and of Q band between 630 and 660 nm, see Table 1), to avoid any enhancement of the second order NLO response due to resonance. The incident beam was obtained by Raman shifting the 1064 nm emission of a Q-switched Nd:YAG laser in a high pressure hydrogen cell (60 bar). A liquid cell with thick windows in the wedge configuration was used to obtain the Maker fringe pattern (harmonic intensity variation as a function of liquid cell translation). In the EFISH experiments the incident beam was synchronized with a DC field applied to the solution, with 60 and 20 ns pulse duration respectively in order to break its centrosymmetry. From the concentration dependence of the harmonic signal with respect to that of the pure solvent, the second order NLO response was determined (assumed to be real because the imaginary part was neglected) from the experimental value γ_{EFISH}, through equation (2):

$$\gamma_{EFISH} = \frac{\mu\beta_{\lambda}(-2\omega;\omega,\omega)}{5kT} + \gamma_0(-2\omega;\omega,\omega,0) \qquad (2)$$

where γ_{EFISH} is the sum of a cubic electronic contribution $\gamma_0(-2\omega; \omega, \omega, 0)$ and of a quadratic orientational contribution $\mu\beta_{\lambda}(-2\omega; \omega, \omega)/5kT$, being μ the ground state dipole moment, and β_{λ} the projection along the dipole moment direction of the vectorial component β_{vec} of the tensorial quadratic hyperpolarizability working with the incident wavelength λ.

The $\mu\beta_{1907}$ values reported in Table 1 are the mean values of twelve successive measurements performed on the same sample. The sign of $\mu\beta_{1907}$ was determined by comparison with the reference solvent and the value from experimental γ_{EFISH} neglecting the cubic electronic

contribution $\gamma_0(-2\omega;\ \omega,\ \omega,\ 0)$, since the porphyrinic chromophores under investigation are characterized by a high dipolar contribution to γ_{EFISH}.[27]

All experimental EFISH $\mu\beta_{1907}$ values are defined according to the "phenomenological" convention.[28] EFISH experiments were carried out in the Department of Chemistry of the University of Milano (Italy).

DFT and CP-DFT calculations

At theoretical level, solvation effects can be treated by means of polarized continuum models (PCMs),[29,30] describing the solvent as a structure-less medium, characterized by its own dielectric constant, and the solute as a molecule embedded in a cavity in the continuum. The role of solvent in treating excited state properties such as electronic absorption and emission energies through PCMs approaches has been extensively investigated by means of TDDFT calculations,[31] evidencing the importance to include the effects of the reciprocal solvent/solute polarization to get a better agreement with experimental findings, in particular when treating polar solvents. On the contrary, not conclusive statements on the appropriateness of PCMs in describing solvent effects on the NLO response have been provided,[32-35] probably owing to its complex dependence on the ground and excited states dipole moments, in both magnitude and relative orientation, the transition dipole moments and the excitation energies, where more than one excited state could be involved. Each of such factors could experience in different way the effect of the surrounding medium. Masunov and coworkers in their theoretical investigation on NLO second-order response of D/A-substituted benzenes and stilbenes[32] concluded that bulk solvent effects can be neglected because their inclusions by means of PCM approaches produce variations comparable with the experimental uncertainty. Moreover, previous investigations performed by some of us

on 5,15 *meso* diaryl Zn^{II} porphyrinates indicated that even a better match with NLO experimental quantities is obtained by performing *in vacuo* calculations.[10,13,15]

In the present investigation, the NLO response of porphyrinates DMF solutions put in evidence even more subtle solvent effects due to explicit solute-solvent interactions, which are obviously neglected in PCMs approaches. Taking into account all the above considerations, we decided to perform all calculations *in vacuo*, optimizing the geometries of both the isolated porphyrins and all their aggregates which are hypothesized to be present in solution, including the adducts with DMF, according to a supermolecule approach.

All calculations were performed by the Gaussian09 program package.[36] According to previous theoretical investigation on similar porphyrinic derivatives,[10] the B3LYP functional[37] and the 6-311g(d)[38] basis set were first adopted to investigate the geometrical and electronic properties of monomers and aggregates. Subsequently, we became aware that the B3LYP functional, while suitable to investigate monomers, electrostatics-dominated hydrogen-bonded dimers and chromophores interacting with DMF, was not appropriate for dimeric J-aggregates, which are supposed to be largely dominated by interchromophoric $\pi-\pi$ stacking interactions besides local interactions between the metal ion and the pendant polar groups ($-N(CH_3)_2$ or $-COOH$/$-COOCH_3$) of the adjacent porphyrinic unit. Recent theoretical investigation on simple porphyrinic aggregate[39] indicated the B97D functional, able to describe dispersion contributions to the interaction, as the most appropriate one to compute the full potential energy surface of these aggregates, which were then confirmed to be mainly of dispersive nature. In the case of our Zn^{II} porphyrinates, we deemed more suitable the dispersion-corrected TPSS-D3 functional,[40,41] owing to its additional advantage to be one of the best performing DFT functional for transition metal chemistry,[42,43] including investigation of stacking interactions of square-planar metal

complexes.[44] This functional was therefore chosen for geometry optimization of dimeric J-aggregates and evaluation of their interaction energies (ΔE), while B3LYP was used for all the other systems. As a check of the internal consistency of the results obtained with the two functionals, we selected one system lacking in π stacking interactions, i.e., the hydrogen bonded dimer of **1** with DMF (**1·DMF HB**, Table 2) and performed geometry optimization using B3LYP and TPSS-D3. The interaction energies obtained in the two cases were ΔE = -56.9 and -64.4 kJ/mol, respectively. While non-negligible in absolute terms, such difference can be judged not significant for the purpose of comparing each other different types of aggregates, which resulted to be characterized by quite different ΔE ranges.

The effect of basis set superposition error (BSSE) was evaluated in the case of complex **1**, whose optimized adduct hydrogen-bonded with DMF (**1·DMF HB**, Table 2), and head-to-head J-aggregate (**1·1(J$_{hh}$)**, Table 2), were submitted to a standard counterpoise calculation to provide a ΔECP interaction energy devoid of BSSE. In spite of the use of a rather extended triple-ζ valence basis set, a relatively high difference between ΔE and ΔECP values was obtained for the two dimers (-56.9 *vs.* -50.7 kJ/mol, respectively, for **1·DMF HB**, and -209.9 vs. -178.9 kJ/mol, respectively, for **1·1 (J$_{hh}$)**). The difference was higher for the dimeric J-aggregate with respect to the DMF hydrogen-bonded species (15% vs. 11%, respectively) owing to a much larger area of overlap in the former case. Such analysis therefore indicates that the calculated ΔE values reported in Table 2 represent a significant overestimate of the true interaction energies, in particular for J-aggregates.

Hyperpolarizabilities were computed by coupled-perturbed (CP) B3LYP/6-311g(d) procedures at the same frequency used in the experimental measurements (1907 nm) and are reported according to the phenomenological convention.[28]

^{1}H PGSE NMR

^{1}H PGSE NMR measurements were carried out on compounds **2** and **5** at 296 K without spinning on a Bruker DRX 400 spectrometer equipped with a QNP probe with a Z-gradient coil and a GREAT 1/10 gradient unit by using the standard stimulated echo sequence. The dependence of the resonance intensity I on a constant waiting time and on a varied gradient strength (G) is described by equation (3) as:

$$\ln \frac{I}{I_0} = -(\gamma\delta)^2 D_t \left(\Delta - \frac{\delta}{3}\right) G^2 \qquad (3)$$

where I_0 is the resonance intensity in absence of the gradient, γ is the magnetogyric ratio, D_t is the translational self-diffusion coefficient, Δ is the distance between the midpoint of the gradients and δ is the length of the gradient pulse. The shape of the gradient pulse was rectangular, the length was 4–5 ms and their strength G was varied during the experiment. All spectra were acquired with a resolution of 32K points and a spectral width of 5000 Hz and processed with a line broadening of 1.0. The semilogarithmic plots of $\ln(I/I_0)$ versus G^2 were fitted by means of a standard linear regression algorithm, obtaining a correlation factor value better than 0.99 in all cases. Different values of Δ, G and number of transients were used in different experiments.

The self-diffusion coefficient D_t, which is directly proportional to the slope of the regression (*m*) obtained by fitting the $\ln(I/I_0)$ versus G^2 plot, was estimated by evaluating the proportionality constant for a sample of HDO (5%) in D_2O (known diffusion coefficients in the range 274–318 K)[45,46] under the exact same experimental conditions as the sample of interest. Tetrakis-(trimethylsylil)sylane (TMSS) was used as internal standard to account for possible changes in the solution viscosity, temperature and absolute gradient strengths.[47] The D_t values were treated to obtain hydrodynamic dimensions as described in the literature. The measurement uncertainty

was estimated by determining the standard deviation of *m* performing experiments with different Δ values and error propagation analysis yielded a standard deviation of 3–4% in the P parameter for all the solutions having a concentration larger than 10^{-5} M. For less concentrated solutions, the standard deviation approaches 5–8%.

Results and discussion

Synthesis

The synthesis of the second order NLO chromophores **1**, **2**, **3**, **4**, **6** and **7** was carried out as reported elsewhere by some of us.[15,16,26] The synthesis of **2bis** followed a procedure reported in the literature (see Scheme S1 and experimental details in the SI),[48] consisting in the esterification reaction of **2** with (Trimethylsilyl)diazomethane, while the synthesis of **5** was realized by means of a two-step approach, as described in the literature,[10] and involved the preparation of the intermediate **10** (see Scheme S2 and experimental details in the SI).

Commercially available 4-Bromo-1,8-naphthalic anhydride was reacted with (Trimethylsilyl)diazomethane in a 2/1 mixture of THF/CH_3OH, working at room temperature, affording after chromatographic purification 1-Bromo-4,5-carboxymethyl-naphthalene (**8**) in high yield (82%).[48] Through a Sonogashira coupling reaction, the (Trimethylsilyl)ethynyl fragment was then introduced, affording **9** in almost quantitative yield. Deprotection of the Trimethylsilyl group in basic conditions (K_2CO_3) led in almost quantitative yield to the intermediate **10**, which was used for the synthesis of the porphyrinic chromophore **5** following a synthetic two-step pathway (Scheme 3 and experimental details in the SI).

A first Sonogashira coupling reaction between [5,15-Diiodo-10,20-bis(3,5-di-*tert*-butylphenyl)porphyrinate]Zn^{II} [15] and **10** afforded after chromatography the intermediate **11**. A

further Sonogashira coupling between this latter and 4-Ethynyl-N,N-dimethylaniline led to **5** (62% yield).

Electronic absorption spectroscopy

The electronic absorption spectra of **1-7** recorded in $CHCl_3$ and DMF solution and normalized with respect to the maximum absorption wavelength of the B band are reported in Figures S1 and S2 (SI), respectively. Moreover, for chromophore **2** the absorbance *vs* concentration dependence spectra in $CHCl_3$ and DMF are reported in Figures S3 and S4.

The experimental λ_{max} of the B and Q bands in $CHCl_3$ and DMF are collected in Table 1, while those in THF solution were already reported in the literature.[13,14,24]

Table 1. Absorption data of B and Q bands in $CHCl_3$, DMF and THF solution, and EFISH $\mu\beta_{1907}$ values in DMF and in $CHCl_3$ as a function of concentration of chromophores **1-7**.

Chrom.	λ_{max} *[logε]* (nm) $CHCl_3$	λ_{max}*[logε]* (nm) DMF	λ_{max} *[logε]* (nm) THF	$\mu\beta_{1907}$ (x10^{-48} esu) DMF	$\mu\beta_{1907}$ (x10^{-48} esu) $CHCl_3$
1	448*[5.40]*[a] 633*[4.33]*[b]	448*[4.61]*[a] 665*[3.38]*[b]	451*[5.48]*[a,c] 659*[4.68]*[b,c]	-1600[f] -3055[g] -3320[h]	-215[g]
2	449*[4.86]*[a] 656*[4.23]*[b]	452*[4.90]*[a] 670*[4.21]*[b]	456*[5.23]*[a,c] 671*[4.69]*[b,c]	-1720[f] -2520[g] -3010[h]	-670[g] -970[h]
2 bis	447*[5.21]*[a] 645*[4.25]*[b]	454*[5.49]*[a] 676*[5.00]*[b]	nd	-1080[f] -1096[g]	-357[g]
3	449*[4.58]*[a] 650*[3.86]*[b]	450*[4.67]*[a] 676*[4.07]*[b]	454*[5.00]*[a,c] 673*[4.51]*[b,c]	-4180[f] -7470[g] -7940[h]	-830[g]

4	450[a] 647[b]	452[a] 667[b]	451*[5.32]*[a,d] 662*[4.61]*[b,d]	-490[f]	-457[g]
5	454[a] 658[b]	460[a] 684[b]	461[a] 678[b]	-1240[f] -1490[g]	 +586[g]
6	454[a] 650[b]	457[a] 671[b]	459*[5.47]*[a,e] 667*[4.89]*[b,e]	+1030[f]	+2978 ($5x10^{-5}$M)
7	439[a] 566[b] 606[b]	443[a] 579[b] 619[b]	439*[5.18]*[a,d] 573*[4.15]*[b,d] 613*[3.94]*[b,d]	+520[f]	+550[g]

[a]λ_{max} of the B band. [b]λ_{max} of the Q band. [c]From ref. 15. [d]From ref. 16. [e]From ref. 26. [f]10^{-3}M solution. [g]$5x10^{-4}$M solution. [h]10^{-4} M solution.

The electronic absorption spectra of **1-6** show the typical pattern of 5,15 push-pull diaryl Zn^{II} porphyrinates,[7-10] consisting in a very strong band at about 450 nm (B band), and only one quite strong band in the range 600-700 nm (Q band). On the other hand, the electronic absorption spectrum of **7** displays two rather weak Q bands, in accordance to the four orbital model of Gouterman,[49] as previously evidenced by some of us.[16]

For all the chromophores the λ_{max} of the B band is rather similar in the three investigated solvents (within a range of 7 nm, Table 1). Differently from the B band, the Q band λ_{max} at lower energy, originated by the HOMO-LUMO transition, span a wider range of wavelengths in both $CHCl_3$ and DMF solution. For instance in $CHCl_3$ the value of λ_{max} follows the sequence **1** << **2 bis** ≈ **4** < **3** < **2** ≈ **5**. The marked red shift observed by the substitution of the weak electron donor $–OCH_3$ group with the stronger donor $–N(CH_3)_2$ group is in agreement with a reduction of the HOMO-LUMO gap typical of 5,15 push-pull diaryl ZnII porphyrinates.[13]

Moreover, when two $-COOCH_3$ acceptor groups are connected to the porphyrinic ring by a naphthalenic unit as in **5**, the λ_{max} of both B and Q bands are significantly shifted at higher wavelengths in all the three investigated solvents (Table 1).

For all the chromophores **1**-**6** a marked red shift of the Q band occurs going from $CHCl_3$ to THF and DMF solutions, as expected for the strong electron transfer character of this Q band,[13] quite sensitive to the solvent polarity, an effect already reported for the electronic absorption spectra of [5,10,15,20-tetraphenylporphyrinate]Zn^{II}.[50]

In accordance, comparing **1** and **2**, the higher difference of λ_{max} of the Q band ($\Delta\lambda_{max}$ = 23 nm) occurs in $CHCl_3$, while it is less relevant in a basic solvent like THF ($\Delta\lambda_{max}$ = 12 nm),[15] and much less relevant in DMF solution ($\Delta\lambda_{max}$ = 5 nm) (Table 1).

Quite unexpectedly the introduction of four fluorine atoms in the acceptor part of the push-pull system as in **3** has a very limited effect on the λ_{max} value of both B and Q bands compared to **2**. This could be due to the proposed tilted arrangement in **3** of the fluorinated aromatic ring with respect to the porphyrinic core, that lowers the conjugation of the push-pull system.[15]

The observed significant differences of λ_{max} of the Q band for chromophores **1-5** in $CHCl_3$, THF and DMF solution can suggest a solvent effect due to the presence of aggregation processes which may be different in the three solvents. This is in agreement with our previous investigation[10] reporting that 5,15 push-pull metal diaryl porphyrinates like **6** form in solution dimeric aggregates whose nature strongly depends on the solvent ($CHCl_3$ or DMF). This seems to be a property of this kind of dipolar pseudo 2D push-pull porphyrinic structures, while such dimeric aggregation does not appear to be typical of a more hindered push-pull 3D structure like **7**. In fact, for this latter chromophore the difference of λ_{max} of the B band and in particular of the two Q bands in the three different solvents is less significant.

EFISH and theoretical investigation of the second order NLO properties of chromophores 1-7

The EFISH data in DMF and in $CHCl_3$ solution are reported in Table 1. The dipolar architecture of **1-5** (Chart 1) and the solvatochromism of their Q band characterized by a red shift of λ_{max} by increasing the polarity of the solvent (Table 1) would suggest at first view a positive second order NLO response, as also supported by CP-DFT calculations *in vacuo* (Table 2), which provided for all chromophores **1-5** positive values of $\beta_{\|}$, being $\beta_{\|}$ the projection of the tensor $\boldsymbol{\beta}$ along the dipole moment axis.

Therefore, the *negative* values of $\mu\beta_{1907}$ experimentally recorded for **1-4** in DMF and $CHCl_3$ and for **5** in DMF are quite unexpected, taking into consideration that under similar experimental conditions the $\mu\beta_{1907}$ value of **6** is always positive.

It thus appears that with a –COOH or $–COOCH_3$ acceptor group, either in a polar and donor (DMF) or in scarcely polar and acidic ($CHCl_3$) solvent, an inversion of the sign of the EFISH response $\mu\beta_{1907}$ occurs independently on the nature of the donor group ($-OCH_3$ or NMe_2). Interestingly such an inversion does not occur for the naphthalenic diester **5** in $CHCl_3$ and neither in DMF nor in $CHCl_3$ solution for **7**, characterized by a push-pull structure at 2,12 β-pyrrolic positions. This latter observation would suggest that the negative $\mu\beta_{1907}$ values of **1-5** and **2bis** may be related to the presence of various aggregates involving the –COOH or $–COOCH_3$ acceptor groups of their less sterically hindered structure, which is reported to structurally favor in solution specific dimeric aggregates.[10]

The critical role of –COOH or $–COOCH_3$ groups is also confirmed by the evidence that the $\mu\beta_{1907}$ absolute values of **1-3** are quite dependent on the nature of the solvent, since they are significantly lower in $CHCl_3$ than in DMF solution, a trend just opposite to that of **6**.

Moreover the presence of a –COOH or even a $–COOCH_3$ group in the structure of the investigated porphyrinates may be responsible of the formation of aggregates of different nature and, in the case of the –COOH group, also of additional acid-base interaction with a basic solvent like DMF.

The intermolecular aggregation of porphyrinic chromophores was extensively studied by Ray and Leszczynski,[51] who showed by a ZINDO/CV computation approach that the quadratic hyperpolarizability of J-type aggregates is several times higher than that of monomers, while for H-type aggregates its value decreases due to the antipodal arrangement of the dipoles of the two molecules forming the aggregate. Moreover, dimers are only a first step of the aggregation in solution, since the presence of higher aggregates cannot be excluded, depending on the NLO chromophores, on the concentration and on the nature of the solvent.

The presence of a –COOH instead of $–NO_2$ acceptor group may stabilize additional dimeric aggregates by intermolecular acid-base interactions of the –COOH group and the Zn^{II} acidic centre with the $–N(CH_3)_2$ basic group of two adjacent chromophores. Moreover in DMF, for both monomeric and dimeric chromophores, the apical or hydrogen bonded acid-base interaction of the -COOH group or of the Zn^{II} centre with DMF, and the 1:1 cyclic interaction of the -COOH groups may be important.

In particular, we may have (Figure 1, where X indicates the NLO porphyrinic chromophore) **(a)** head-to-head, $X{\cdot}X(J_{hh})$ or head-to-tail $X{\cdot}X(J_{ht})$ dimeric J-aggregates, and head-to-tail dimeric H-aggregates, the latter being however less stable owing to the implied overlap of the bulky *tert*-butylphenyl groups; **(b)** centrosymmetric 1:1 hydrogen bonded dimers involving the –COOH groups of two chromophores, X·X(HB); **(c)** in DMF only, acid-base interactions of DMF with either the acidic Zn^{II} center, $X{\cdot}DMF_{apical}$, and/or the -COOH group by hydrogen bond, $X{\cdot}DMF_{HB}$,

which compete with J-aggregates and with the X·X(HB) dimers, respectively. The hydrogen-bonded interaction with DMF may occur also for the X·X(J_{hh}) dimeric aggregate. In the case of **4**, the formation of larger aggregates consisting in a complex array of intermolecular hydrogen-bonded interactions involving the two –COOH groups should also be taken into account.

Figure 1. Schematic representation of possible species in $CHCl_3$ and DMF solution

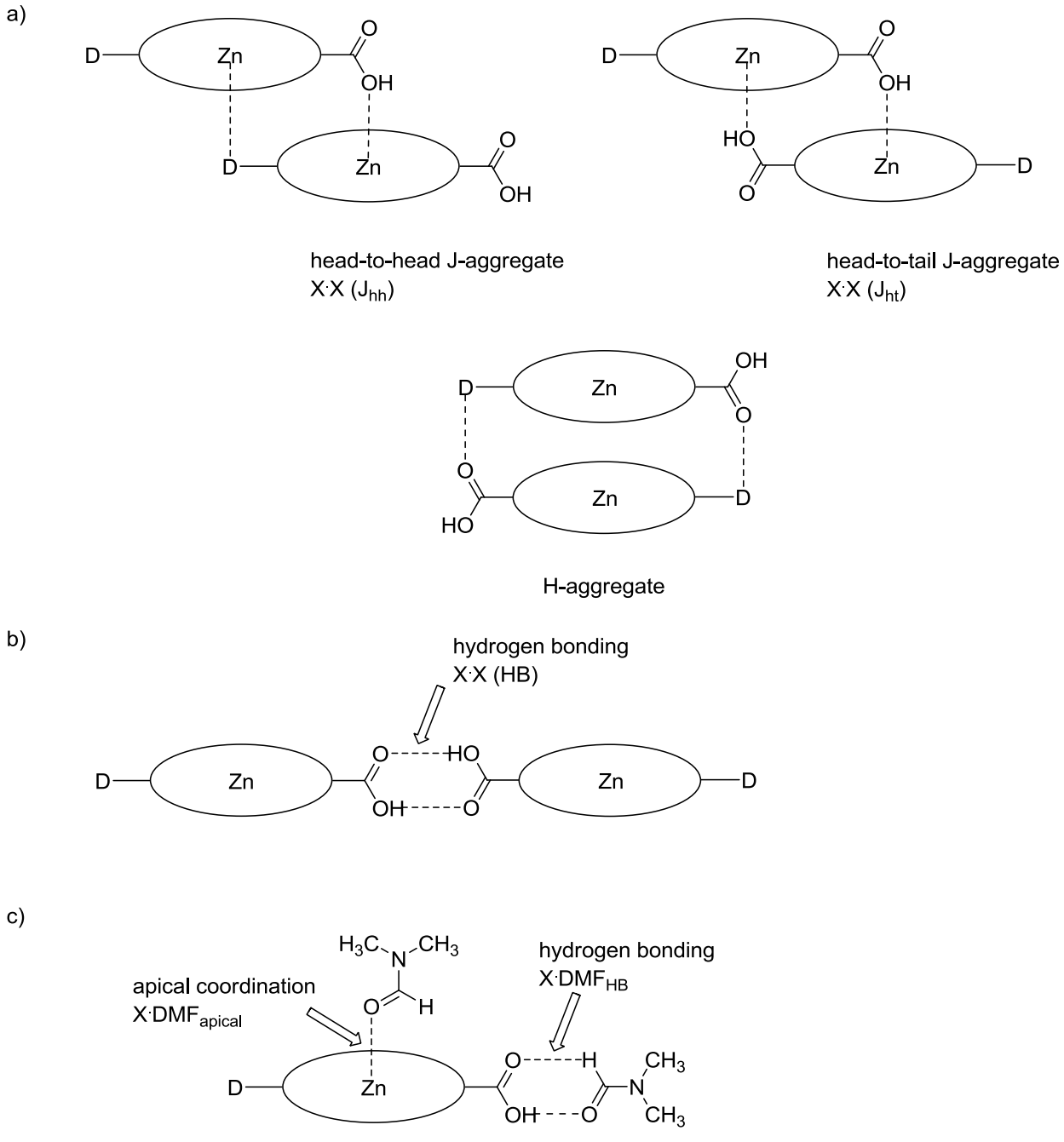

The relative energetic stabilization of the various possible species of **1-5**, **2bis** and **6** in $CHCl_3$ and in DMF has been evaluated by DFT calculations on selected X·X self-aggregates and X·DMF dimeric species. Calculations were performed *in vacuo* as previously done for structurally related push-pull metal porphyrinates.[10,13,15] It should be taken into account that the adopted computational approach overestimates by about 10-15% the interaction energies owing to Basis Set Superposition Error (see the details of DFT and CP-DFT calculations in the Experimental).

Table 2. In *vacuo* computed dipole moments (μ) and projection of the dynamic tensor β along the direction of the dipole moment ($\beta_{\parallel}$) for chromophores **1-6** and for a selection of their possible J aggregates and adducts with DMF, together with the relative interaction energies[a]

X	μ (D)	$\beta_{\parallel}$ ($x10^{-30}$ esu)	Interaction energies (kJ/mol)
1	5.22	132	–
1·1 (J_{hh})	11.53	nd	-209.9
1·1 (HB)	0.22	nd	-78.3
1·DMF_{HB}	2.98	-24	-56.9
1·DMF_{apical}	6.62	88	-51.8
(1·DMF_{HB})·(1·DMF_{HB})(J_{hh})	4.02	-65	-242.6
2	8.66	259	–
2·2 (J_{hh})	15.86	nd	-237.9
2·DMF_{HB}	3.08	180	-56.1
2·DMF_{apical}	11.54	210	-50.7
(2·DMF_{HB})·(2·DMF_{HB}) (J_{hh})	4.00	nd	-271.9

2bis	7.86	247	–
2bis·DMF_{HB}	3.05	234	-18.7
2bis·DMF_{apical}	8.27	191	-50.5
3	10.53	342	–
3·3 (J_{hh})	19.99	nd	-252.1
3·DMF_{HB}	4.07	249	-55.7
(3·DMF_{HB})·(3·DMF_{HB}) (J_{hh})	5.99	Nd	-291.5
4	10.16	230	–
4·4 (HB)	0.37	nd	-78.9
4·DMF_{HB}	4.56	214	-58.2
4·2DMF_{HB}	4.33	15	-103.3
5	7.98	256	–
5·DMF_{apical}	11.02	nd	-51.1
6	10.37	244	–
6·6 (J_{hh})	20.72	nd	-200.4

[a] μ and $\beta_{\|}$ evaluated at the B3LYP/6-311(d) and CP-B3LYP/6-311(d) levels of theory, respectively. Geometry optimization and interaction energies at the B3LYP/6-311(d) level of theory except for J-aggregates, for which the TPSS-D3/6-311(d) level has been adopted.

According to Table 2, very large values (up to 290 kJ/mol) were computed for X·X (J_{hh}) aggregates, quite dependent on the nature of the donor and acceptor groups of the push-pull system. In particular, the –COOH group appears to play a key role, giving rise to a more stable J-aggregation than the -NO_2 group (for example, compare the dimerization energy calculated for the **2·2 (J_{hh})**, -237.9 kJ/mol, with that of **6·6 (J_{hh})**, -200.4 kJ/mol). The strength of such aggregation is further enhanced when each –COOH group of the J_{hh} aggregate is hydrogen-

bonded with DMF (see in Table 2 the increased interaction energies computed for the $(X{\cdot}DMF_{HB}){\cdot}(X{\cdot}DMF_{HB})(J_{hh})$ species of **1**, **2** and **3** when compared to $X{\cdot}X(J_{hh})$).

Since previous investigation[10] indicated that J_{hh} and J_{ht} aggregates of this kind of 5,15 push-pull diaryl Zn^{II} porphyrinates are almost isoenergetic, calculations of the dimerization energy of $X{\cdot}X$ (J_{ht}) aggregates were not carried out.

Much lower interaction energies were computed for the centrosymmetric X·X (HB) hydrogen-bonded dimers (about 75 kJ/mol) and even lower for the $X{\cdot}DMF_{HB}$ acid-base species (about 54 kJ/mol, Table 2).

Obviously the substitution of the –COOH group with the less acidic $–COOCH_3$ group induces a much lower energetic stabilization of the hydrogen-bonded adduct with DMF (-18.7 kJ/mol for **2bis**$\cdot$**DMF$_{HB}$** in comparison to -56.1 kJ/mol for **1**$\cdot$**DMF$_{HB}$**) (Table 2).

The dimerization process leading to H-aggregate was not evaluated because, as above pointed out, it is expected to be strongly disadvantageous due to the repulsion of the *tert*-butyl groups on the two aryl moieties in 10,20 position of the chromophore ring, despite the favored dipole-dipole orientation of the two adjacent head-to-tail chromophores (Figure 1).

It must be taken into account that the formation of dimeric aggregates induces a substantial geometrical deformation of the structure of the two interacting chromophores, so that the associated dipole moments are not doubled or vanishing (for the J_{hh} and J_{ht} dimers, respectively) with respect to the dipole moments of the monomeric species.

The computed energy differences would suggest the presence in solution of significant amounts of J_{hh}- and/or J_{ht} aggregates, together with a limited amount of 1:1 symmetrical hydrogen bonded dimers ($X{\cdot}X$(HB)) mainly at higher concentration. The relative concentration of these species should produce significant effects on the EFISH second order NLO response of

the chromophores. On the other hand, the weak acid-base hydrogen-bonded interaction of monomeric chromophores or J_{hh} dimers with DMF is not expected to influence the hyperpolarizability, but it may imply a significant change (in both direction and magnitude) of the dipole moment and therefore of the sign and magnitude of $\mu\beta_{1907}$ (see for instance the negative $\beta_{\parallel}$ values computed for monomeric **1**·**DMF$_{HB}$** and dimeric (**1**·**DMF$_{HB}$**)·(**1**·**DMF$_{HB}$**)(**J$_{hh}$**) species, Table 2).

Starting from the above considerations and evidences, a reasonable interpretation of the origin of the intriguing experimental EFISH $\mu\beta_{1907}$ data can be attempted:

i) The relatively low $\mu\beta_{1907}$ absolute value of **1-3** in $CHCl_3$ solution and for **2** also slightly dependent from concentration could be an evidence of the parallel presence of some concentration-dependent NLO-silent X·X (HB) dimers or of [(X·X)(J_{hh})·(X·X)(J_{hh})] (HB) higher aggregates, and of significant amounts of stable, less concentration dependent NLO active X·X(J_{hh}) aggregates. The significant presence of these latter species in the case of **1-3** is supported by the positive and rather low $\mu\beta_{1907}$ value in $CHCl_3$ of **5**, for which the absence of a –COOH group and the presence of a naphthalenic π system should make less stable the J_{hh} dimers, favoring the presence in solution mainly of monomeric chromophores which are expected to produce a positive NLO response, as it was reported to occur for **6**, lacking the –COOH group.[10]

Further evidence of the role of the –COOH group in stabilizing the J_{hh} dimers in $CHCl_3$ solution of **1-3** is the lower absolute value of $\mu\beta_{1907}$ of **2bis** with respect to that of **2**, given that the substitution of the –COOH with the $–COOCH_3$ group should provide less strong intermolecular interactions.

Interestingly, infrared measurements of a rather concentrated $CHCl_3$ solution of **2** confirmed the proposed presence of NLO silent X·X(HB) dimers, showing a band at 1686 cm^{-1}, which can

be ascribed to the –C=O stretching of the 1:1 species.[52] Such interaction may involve not only the monomeric chromophores, but probably also their J_{hh} aggregates, **2**·**2(J$_{hh}$)**, to produce higher aggregation through the free –COOH group ([(X·X)(J_{hh})·(X·X)(J_{hh})] (HB) species). The presence at higher concentrations of NLO-silent X·X(HB) dimers is also supported by the slight increase of the $\mu\beta_{1907}$ value of **2** by dilution (Table 1), due to an increase of NLO active J_{hh} aggregates, as an effect of the breaking off by dilution of the less stable NLO silent X·X(HB) dimers. As we will see later, such interpretation has been confirmed by self-diffusion ^{1}H-NMR measurements.

ii) In DMF solution, negative $\mu\beta_{1907}$ are as well recorded for **1**-**5**, characterized with the exception of **4** by absolute values much higher than those in $CHCl_3$ (Table 1). Moreover, a more pronounced concentration effect occurs for **1**, **2** and **3**, since their $\mu\beta_{1907}$ absolute values strongly increase by dilution. This behavior is controlled by the –COOH group, since **2bis** and **5** do not show any dilution effect in the same range of concentration (Table 1), suggesting the presence at high concentration of some amounts of NLO-silent [(X·X)(J_{hh})·(X·X)(J_{hh})] (HB) species. Dilution induces the breakdown of such higher aggregates, thus producing a relative increase of the concentration of the NLO active X·X(J_{hh}) dimers. The only exception is chromophore **4**, the low $\mu\beta_{1907}$ value of which does not depend neither on concentration nor on the solvent (Table 1), suggesting the formation of low polar, highly stable higher aggregates.

Since the $\mu\beta_{1907}$ absolute values of **1**-**3** are much higher in DMF than in $CHCl_3$ solution (Table 1), we can suggest the presence in DMF of higher amounts of stable NLO active X·X(J_{hh}) aggregates, further stabilized by the acid-base hydrogen bonding of the –COOH group with DMF. The key role of the -COOH group in inducing a high stability to X·X(J_{hh}) dimeric aggregates in DMF is a crucial observation because their formation in DMF was denied for a slightly different push-pull diaryl Zn^{II} porphyrinate such as **6**.[10]

The much higher $\mu\beta_{1907}$ absolute value of **3** even at a relatively high concentration confirms an increased stability of the J_{hh} dimers due to a quite strong –COOH/DMF interaction, owing to the increased acidity given by the four fluorine atoms (Table 1).

In general both in $CHCl_3$ and DMF solution the key role of the –COOH in stabilizing J_{hh} aggregates for chromophores **1**-**3** is confirmed by the quite different EFISH response of the more compact and sterically hindered chromophore **7**. In this latter, the presence of four aryl groups in the 5,10,15,20 *meso* positions of the porphyrinic core and the push-pull system involving the 2,12 β-pyrrolic positions (Chart 1) do not allow J_{hh} aggregations and at the same time hinders the formation of symmetrical 1:1 hydrogen bonded dimeric aggregates. As a consequence, the EFISH $\mu\beta_{1907}$ value of **7** is positive, low and not dependent on the nature of the solvent and on dilution (Table 1), and corresponds to the intrinsic NLO response of the monomer, as expected for the lack of significant intermolecular aggregations and solvation effects.

iii) DMF appears to play a key role in determining the negative sign of the second order NLO response of chromophores **1-5**. On one side, the relatively weak DMF apical coordination to the central Zn^{II} ion of monomeric or of dimeric J_{hh} aggregate of chromophores **1-3** should not produce an appreciable influence on the second order NLO response,[53] as confirmed by the theoretical DFT and CP-DFT calculations (Table 2). On the other side, the DMF molecule hydrogen-bonded to the -COOH group of the chromophore (either as a monomer or as a J_{hh} dimeric aggregate) is expected to strongly modulate the dipole moment of the newly formed hydrogen-bonded species, owing to its arrangement just along the push-pull molecular axis. As previously reported from both an experimental and theoretical point of view,[3,54-57] such a local interaction of the chromophore with solvent molecules may even produce an inversion of the

dipole direction, while keeping unvaried the direction of charge transfer in the excited state, so as to generate a negative $\mu\beta_{1907}$ response.

For instance, an inversion of sign of $\mu\beta_{1907}$ going from $CHCl_3$ to DMF solution was previously reported for an halogenated second order NLO chromophore and was ascribed to halogen bonding interaction between the chromophore and DMF.[58] Here DFT and CP-DFT calculations indicate that this seems to be exactly the case of **1**, whose acid-base hydrogen bonded species with DMF, **1·DMF$_{HB}$**, shows a computed negative $\mu\beta_{\|}$ value, an evidence further provided by its DMF hydrogen bonded dimeric J_{hh} aggregate (**1·DMF$_{HB}$**)·(**1·DMF$_{HB}$**) **J_{hh}** (Table 2). However, such rationale is not fully confirmed by our calculations on chromophores **2** and **3**, for which only a strong reduction in the dipole modulus was obtained after interaction with DMF molecules (**2·DMF$_{HB}$** and **3·DMF$_{HB}$** dimers). The dipole orientation, on the other hand, is essentially unvaried, so that positive $\mu\beta_{\|}$ products are obtained for these hydrogen-bonded species, at variance with the experimental findings. A possible reason of such disagreement for compounds **2** and **3** could be found in the neglecting of polarizing effects of the medium, which are expected to be significant and very specific for large dimeric J_{hh} aggregates, so that they can strongly influence the orientation of dipole moments, particularly if they are small.

Interestingly, such disagreement persists even including in calculations the polarizing effects of the medium by means of PCMs,[29,30] confirming the previously reported doubts on the appropriateness of these methods to model the NLO response in solution of large porphyrinic systems.[10,13,15] This would suggest the need of adopting more sophisticated approaches, able to properly describe the concomitant effect on NLO properties of both polarizing effects and specific solute-solvent interactions, which could locally modify dipole moment, polarizability and geometry of solvent molecules and hence the dielectric constant.

It appears that probably the inversion of sign of the second order EFISH NLO response of **1-3** can be ascribed in DMF solution to strong, specific and complex solvation effects, which become relevant in the presence of a free –COOH groups. Interestingly, when the –COOH group is substituted by the $–COOCH_3$ group (compound **5**) this inversion is still present in DMF solution, but not in $CHCl_3$ solution. The less polar $CHCl_3$ solvent should produce less important solvation effects on the J_{hh} dimers of **2bis** and **5**, thus reducing its influence on the sign of the second order NLO response. On the other hand, chromophores **1-3**, bearing the –COOH group, may experience significant solvation effects even in a less polar and acidic solvent as $CHCl_3$, thus showing a negative value of the second order NLO response. Of course the role of these significant and specific solvation effects on the sign of the NLO response of **1-3** is at the moment only a suggestion, which must be confirmed by further DFT and CP-DFT calculations using PCMs approaches including inhomogeneous dielectric effects.[30]

^{1}H PGSE NMR measurements

Electronic absorption spectra, EFISH measurements and infrared evidences produce indications that the second order NLO porphyrinic chromophores **1-5** are involved in both $CHCl_3$ and DMF solution in aggregation processes, based on the formation of various dimers and also higher aggregates. Therefore self diffusion experiments were performed with the aim of quantifying the level of self-aggregation in $CDCl_3$ and DMF-d_7 solution of **2** and **5**, taken as a reference of the two types of porphyrinic chromophores investigated in this work. By measuring experimentally the translational self-diffusion coefficient D_t (see the Experimental Section for details), the hydrodynamic dimensions of free diffusing species were evaluated through the

modified Stokes-Einstein equation (4), taking into account the marked asphericity of the molecular structure of **2** and **5**:[59]

$$D_t = \frac{k_b T}{\pi \eta f c \sqrt[3]{a^2 b}} \quad (3) \quad (4)$$

In equation 3, k_b is the Boltzmann constant, T the absolute temperature, η the solution viscosity, f the "shape factor", c the "size factor", while a and b are the semiaxes of the oblate ellipsoid which is considered the best approximation for the shape of **2** and **5**. From the experimental determination of the values of D_t, the structural parameter P of **2** and **5**, defined as $fc\sqrt[3]{a^2 b}$, was thus derived as a function of the concentration and of the fitting model (Table 3).

Table 3. Self-diffusion coefficients (D_t), structural parameters (P), aggregation numbers (N) and dimerization equilibrium constants (K_D) for **2** and **5** in DMF-d_7 (a) and $CDCl_3$ (b)

					Model 1	**Model 2**
	C **(10^{-3}M)**	**D_t** **(10^{-10}m^2 s^{-1})**	**P** **(Å)**	**x_D**	**N** ***(K_D x10^3M^{-1})***	**N** ***(K_D x10^3M^{-1})***
2	0.02[a]	3.20	51.8	0.42	1.42 *(25.0)*	1.30 *(20.0)*
2	0.08[a]	3.07	54.2	0.67	1.67	1.49
2	0.20[a]	3.05	54.5	0.70	1.70	1.52
2	0.80[a]	2.99	55.5	0.80	1.80	1.60
2	0.08[b]	4.93	52.0	0.44	1.44 *(8.7)*	1.31
2	0.7[b]	4.20	61.1	n.a.	>2	2.13
5	0.21[a]	3.12	53.2	0.56	1.56	1.40

					(3.8)	
5	1.66[a]	3.08	53.9	0.63	1.63	1.46
5	0.009[b]	5.25	48.8	0.11	1.11 *(13.0)*	1.08 *(9.0)*
5	0.017[b]	5.19	49.4	0.17	1.17	1.12
5	0.056[b]	4.94	51.8	0.42	1.42	1.29
5	0.18[b]	4.81	53.0	0.54	1.54	1.38
5	1.48[b]	4.53	56.3	0.90	1.90	1.66

The P structural parameters of monomeric **2** and **5** chromophores are computed from their DFT optimized structure *in vacuo*, assuming in first approximation that they have the same dimensions in $CHCl_3$ and DMF solution, despite the significant solvation, at least in DMF. In particular, in the case of **2** the major semiaxis of the ellipsoid (*a*), equal to 10.2 Å, was calculated as the mathematical average of the distances between the central Zn atom and *i)* the methyl group of the dimethylaniline moiety (14.5 Å), *ii)* the farthest CH group of the porphyrinic ring (6.3 Å) and *iii)* the *para*-hydrogen atom of the 3,5-di-*tert*-butylphenyl substituent (9.9 Å) (Figure S3 in the SI).

The estimation of the value of the minor semiaxis (*b*) was not straightforward, owing to the presence of two *tert*-butyl groups on the phenyl ring that, from DFT calculations, appeared to impart a sort of concavity to the structure of the chromophore. Therefore, the *b* value was calculated by extrapolating the P value at infinite dilution; for instance for **5** in $CDCl_3$ (P = 47.7 Å) *b* was found to be equal to 5.1 Å. Such a value is intermediate between the distance from the middle of the aromatic ring and *i)* the farthest methyl group of the *tert*-butyl substituent (5.7 Å) and *ii)* the *ortho* hydrogen atom of the aromatic ring (3.3 Å). For **5** the hydrodynamic volume (V_H) of the monomer was calculated from *a* and *b* values to be 2220 A^3.

From the experimental data reported in Table 3 it appears that P values for both **2** and **5** in $CDCl_3$ and DMF-d_7 solution increase with the concentration, confirming the presence of associative processes of self-aggregation.

In order to quantify the self-aggregation, two different and relatively simple aggregation models were taken into account: 1) an eclipsed head-to-tail π-stacking between two porphyrinic molecules, leading to a H-dimeric aggregate of low dipole moment, and 2) a staggered dimerization that occurs through the intermolecular acid-base interaction of the $–N(CH_3)_2$ group of one chromophore with the Zn atom of an adjacent chromophore leading to the formation of a J_{hh} dimer of high dipole moment. This latter is the model suggested by some of us to occur in $CHCl_3$ solution in the case of **6**.[10] In the case of model 1, the major semiaxis of the dimer can be considered, as a first approximation, equal to that of the monomer (a = 10.2 Å) while the minor semiaxis is increased roughly to 9.5 Å. This leads to an almost spheric dimer with an extrapolated computed P value of 57.5 Å. In model 2, both a and b semiaxes of the pseudo-ellipsoid dimeric structure are different respectively to those of the monomer. The major axis is set equal to 14.2 Å while the minor one to 7.8 Å, giving an extrapolated P value of the dimer of 70.0 Å.

The percentage of dimeric aggregates in $CDCl_3$ and DMF-d_7 solution was thus calculated for both models. For model 1 a monomer-dimer equilibrium was imposed and the percentage of the dimer was calculated from the experimental P values (Table 3) by:

$$P = (1 - x_D)P_M + x_D P_D$$

where x_D is the molar fraction of the dimer and P_M and P_D are the calculated P values for the monomer and the dimer, respectively. From x_D values, the aggregation numbers (N is the ratio of the experimental and the calculated volume of the monomer) was obtained as

$$N = 1 - x_D + 2x_D$$

For model 2 the dimeric aggregate has the same pseudo ellipticity of the monomer, therefore it is possible to calculate directly the aggregation numbers N from the ratio between the experimental P values and the extrapolated P value of the monomer.

From Table 3 it appears that **2** shows a higher tendency than **5** to self-aggregation in $CDCl_3$ even at low concentration, as expected for the presence of the more acidic –COOH group which facilitates aggregation in comparison to the $–COOCH_3$ group. For example, for **2** in the case of model 2, a N value higher than 2 (2.13) was reached already at 0.7 mM concentration in $CDCl_3$ solution, while the aggregation of **5** increased less sharply with the concentration reaching a N value of only 1.66 at a much higher concentration such as 1.48 mM. The same trend but with a less relevant aggregation is observed in DMF-d_7 solution. It follows that, regardless of the model, **2** appears to aggregate more easily, since N values larger than for **5** are calculated at similar concentrations in both $CDCl_3$ and DMF-d_7 solution (Table 3), thus confirming the suggestion reached from the EFISH investigation.

Equilibrium constants and standard free energies associated to the dimeric aggregation process were calculated by interpolating the hydrodynamic data by suitable fitting functions. In model 1, the simple monomer-dimer equilibrium equation was applied and the dimerization constant value (K_D) was derived from x_D and C values. For **2** the calculated value of K_D was 2.5×10^4 M^{-1} in DMF-d_7 ($\Delta G° = –24.7$ kJ/mol) and 8.7×10^3 M^{-1} in $CDCl_3$ ($\Delta G° = –22.2$ kJ/mol). In model 2, N *versus* C values were calculated by using equations derived from indefinite aggregation models.[60] Accurate values of K_D and $\Delta G°$ were obtained only for **2** in DMF-d_7 (2×10^4 M^{-1}) and for **5** in $CDCl_3$ (9×10^3 M^{-1}) since more experimental points were available for the fitting. As expected for a lower tendency to aggregate, the calculated values of K_D of **5** according to model

1 were always lower in both solvents than those calculated for **2**, while not significant differences of calculated K_D values in both solvents are observed for the two models (Table 3).

However, taking into account these rather similar experimental evidences but also the significant theoretically calculated dimerization energies of the J_{hh} aggregate (Table 2), it can be thought that the self-aggregation process of **2** and also of **5** is more likely described in $CHCl_3$ and DMF solution by model 2, in which the dimerization leads to the formation of J_{hh} dimers (Figure 1). The formation of H-type dimeric aggregates corresponding to model 1 can be in any case discounted, despite the above evidence that in model 1 K_D values are higher for both **2** and **5** , because EFISH experiments clearly show a significant second order response of their $CHCl_3$ and DMF solutions (Table 1), which could not be achieved by the symmetrical and therefore rather silent H_{ht} aggregates, considered in model 1. Finally the analysis of the trends of aggregation of **2** and **5**, the N *versus* C values obtained from the experimental data in DMF-d_7 and $CDCl_3$ solution by means of model 2 were plotted (Figure 2).

Figure 2. N versus C trends for chromophores **2** and **5** in $CDCl_3$ and DMF-d7 solution according to model 2

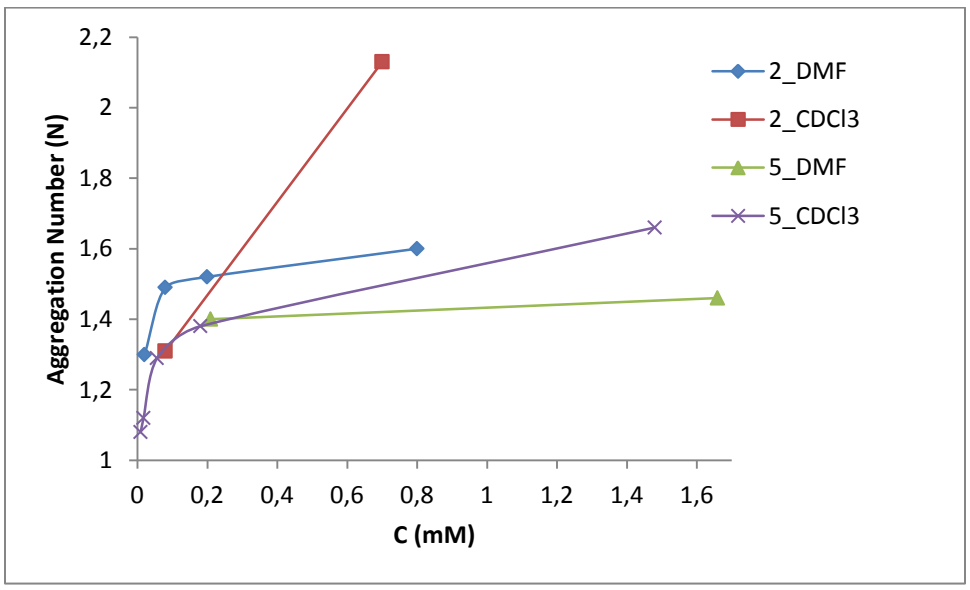

From Figure 2 it can be noted that for both **2** and **5**, regardless of the solvent, the J_{hh} self-aggregation process already starts at rather low concentration ($<10^{-4}$ M). In the presence of a free–COOH group as for the J_{hh}-type dimeric aggregate of **2** (Figure 1) and in a less polar solvent like $CDCl_3$ at relatively high concentration, an additional dimerization motif to form a symmetrical 1:1 hydrogen bonded higher aggregate, may occur. In accordance such a –COOH driven additional dimerization process, not considered in our simple model, leads at higher concentration to an increase of aggregation up to species with N higher than 2 (Table 3 and Figure 2). This process is less relevant in DMF-d_7 solution, where after a significant initial aggregation at very low concentration to form the J_{hh} dimer, the increase of the value of N with concentration is not so relevant (Figure 2), an evidence that the additional –COOH driven higher aggregation of the J_{hh} dimer is quite limited. Such limitation is probably due to the parallel hydrogen bonded interaction of the –COOH group with the excess of DMF, which may reduce the formation of $[(X^{\cdot}X)(J_{hh})^{\cdot}(X^{\cdot}X)(J_{hh})]$ (HB) aggregates.

In the case of chromophore **5**, the dimerization process to form a J_{hh} aggregate occurs initially at very low concentration, but it is less relevant if compared to **2**. Moreover, the value of N does not increase so much by increasing concentration in $CDCl_3$ solution, while it remains constant in DMF-d_7 solution (Figure 2), due to the lack of the –COOH group which makes the J_{hh} dimers more stable and which can produce, as above discussed, higher aggregates.

In conclusion PGSE ^{1}H-NMR experiments confirm an initial significant intermolecular self-aggregation process for both **2** and **5** and in both $CDCl_3$ and DMF-d_7 solution, to produce NLO J_{hh} active dimers, with a stability which follows the order **2** >> **5**, in agreement with the EFISH measurements and with the well estabilished key role of the -COOH group in the self-

aggregation process. Moreover, PGSE experiments highlighted an additional dimerization process to form higher aggregates, which becomes relevant by increasing concentration.

Therefore the significant increase by dilution of the $\mu\beta_{1907}$ EFISH absolute values of **1-3** mainly in DMF (Table 1) is an evidence of the progressive dissociation of these NLO silent $[(X\cdot X)(J_{hh})\cdot(X\cdot X)(J_{hh})]$ (HB) aggregates to form NLO active J_{hh} aggregates, stabilized by hydrogen bond interaction of the free –COOH group with DMF. Such dilution effect is less relevant in $CHCl_3$ solution due to the higher stability in this latter solvent of –COOH driven 1:1 symmetrical hydrogen bonded structures in comparison to DMF, which activates an acid-base competitive interaction with the –COOH group of the chromophore.

Conclusion

Through EFISH measurements, electronic and infrared spectroscopy, DFT and CP-DFT calculations and self-diffusion ^{1}H-NMR experiments, a strong evidence of significant aggregation processes, controlling the second order NLO response both in $CHCl_3$ and DMF solution of 5,15 push-pull diaryl Zn^{II} porphyrinic chromophores, bearing a –COOH group or a –$COOCH_3$ acceptor group and a –$N(CH_3)_2$ or a –OCH_3 donor group has been produced.

It appears that J_{hh} aggregation, strongly stabilized by the –COOH group and much less by the –$COOCH_3$ group, is the most relevant, but another dimerization process still involving the –COOH group occurs as well, with the formation of less stable 1:1 symmetrical hydrogen bonded dimers. Moreover, in DMF the –COOH group of monomeric or J_{hh} dimeric chromophores can be hydrogen bonded with a solvent molecule, with an additional stabilization of the self-dimerization process, particularly in the case of J_{hh} aggregates.

All these –COOH driven interactions are controlled by the dipolar and basic/acid nature of the solvent and by concentration.

A significant solvent effect was already reported by some of us[8] for structurally similar Zn^{II} porphyrinates such as **6**, carrying a $–NO_2$ acceptor group, for which only a J_{hh} aggregation involving acid-base interactions between the basic $–N(CH_3)_2$ group of one chromophore and the Zn^{II} acidic centre of another adjacent one was evidenced.

On the contrary the porphyrinic chromophores investigated in this work are affected by a complex variety of aggregation processes, in which the –COOH group appears to play a key role, since its replacement with a $–COOCH_3$ group produces lower effects in both $CHCl_3$ and DMF solution.

As reported in the literature for example for merocyanine dyes, aggregation by dipole-dipole interaction of second order dipolar dyes can be detrimental, leading to the formation of centrosymmetric species with low $\mu\beta$ values.[61] On the other hand, for other chromophores such as twisted π-electron system chromophores (tictoids), aggregation led to exceptional molecular hyperpolarizabilities.[62]

The present work evidences that another useful strategy to suppress unfavorable aggregation processes in dipolar second order NLO chromophores could be the exploitation of –COOH-driven effects.

Regarding the rather unexpected negative sign of the second order NLO response, DFT calculations suggest that it could be related to specific and strong interactions with the solvent, particularly in DMF solution, due to the presence of the –COOH and $–COOCH_3$ groups.

It also appears that such significant effects are closely related to the pseudo-linear structure of the porphyrinic chromophores, since when the push-pull system is involved in a sterically hindered β-pyrrolic architecture, no effect of the presence of the –COOH group is highlighted.

In conclusion this work has pointed out the great potential of the EFISH technique in disclosing interesting solvent effects (originated for instance by acid-base[10] or dipolar[62] interactions between adjacent chromophores or by solvolysis of coordination compounds induced by the solvent[63]), which can be triggered by a specific molecular substitution and which can strongly affect NLO measurements.

Supporting Information. SI contains the full synthetic details of chromophores **2bis** and **5**; the electronic absorption spectra of **1-7** in $CHCl_3$ and DMF, the absorbance *vs* concentration spectra for **2** in $CHCl_3$ and DMF and additional ^1H PGSE NMR data.

The following files are available free of charge.

ESI_final.pdf

AUTHOR INFORMATION

Corresponding Author

*Francesca Tessore. E-mail: francesca.tessore@unimi.it. Phone: (39) 2 50314397

*Alessandra Forni. E-mail: a.forni@istm.cnr.it. Phone: (39) 2 50314273

Author Contributions

The manuscript was written through contributions of all authors. All authors have given approval to the final version of the manuscript.

Funding Sources

Regione Lombardia − Fondazione Cariplo joint SmartMatLab Project (Fondazione Cariplo grant 2013-1766)

ACKNOWLEDGMENT

The authors deeply thank Prof. R. Ugo for fruitful discussion and for the accurate revision of the manuscript. The use of instrumentation purchased through the Regione Lombardia − Fondazione Cariplo joint SmartMatLab Project (Fondazione Cariplo grant 2013-1766) is gratefully acknowledged.

REFERENCES

(1) Oudar, J. L.; Chemla, D. S. Hyperpolarizabilities of the nitroanilines and their relations to the excited state dipole moment. *J. Chem. Phys.* **1977**, *66*, 2664-2668.

(2) Oudar, J. L. Optical nonlinearities of conjugated molecule. Stilbene derivatives and higly polar aromatic compounds. *J. Chem. Phys.* **1977**, *67*, 446-457.

(3) Abbotto, A.; Beverina, L.; Bradamante, S.; Facchetti, A.; Klein, C.; Pagani, G. A.; Redi-Abshiro, M.; Wortmann, R. A Distinctive Example of the Cooperative Interplay of Structure and Environment in Tuning of Intramolecular Charge Transfer in Second-Order Nonlinear Optical Chromophores. *Chem. Eur. J.* **2003**, *9*, 1991-2007.

(4) Cariati, E.; Pizzotti, M.; Roberto, D.; Tessore, F.; Ugo, R. Coordination and organometallic compounds and inorganic-organic hybrid cristalline materials for second-order non-linear optics. *Coord. Chem. Rev.* **2006**, *250*, 1210-1233.

(5) Di Bella, S.; Dragonetti, C.; Pizzotti, M.; Roberto, D.; Tessore, F.; Ugo, R. Coordination and organometallic complexes as second-order nonlinear optical materials. in *Molecular*

Organometallic Material for Optics – Topics in Organometallic Chemistry Le Bozec H.; Guerchais, V. eds. 2010, *28*, 1-55.

(6) LeCours, S. M.; Guan, H. –W.; DiMagno, S. G.; Wang, C. H.; Therien, M. J. Push-pull arylethynyl porphyrins: new chromophores that exhibit large molecular first-hyperpolarizabilities. *J. Am. Chem. Soc.* **1996**, *118*, 1497-1503.

(7) LeCours, S. M.; DiMagno, S. G.; Therien, M. J. Exceptional electronic modulation of porphyrins through *meso*-arylethynyl groups. Electronic spectroscopy, electronic structure and electrochemistry of [5,15-Bis[(aryl)ethynyl]-10,20-diphenylporphyrinato]zinc(II) complexes. X-ray crystal structure of [5,15-Bis[(4'-fluorophenyl)ethynyl]-10,20-diphenylporphyrinato]zinc(II) and 5,15-Bis[(4'-methoxyphenyl)ethynyl]-10,20-diphenylporphyrin. *J. Am. Chem. Soc.* **1996**, *118*, 11854-11864.

(8) LeCours, S. M.; Phillips, C. M.; de Paula, J. C.; Therien, M. J. Synthesis, transient absorption, and transient resonant Raman spectroscopy of novel electron donor-acceptor complexes: [5,15-Bis[(4'-nitrophenyl)ethynyl]-10,20-diphenylporphyrinato]copper(II) and [5-[[4'-(Dimethylamino)phenyl]ethynyl]-15-[(4"-nitrophenyl)ethynyl]-10,20-diphenylporphyrinato]copper(II). *J. Am. Chem. Soc.* **1997**, *119*, 12578-12589.

(9) Pizzotti, M.; Annoni, E.; Ugo, R.; Bruni, S.; Quici, S.; Fantucci, P.; Bruschi, M.; Zerbi, G.; Del Zoppo, M. A multitechnique investigation of the second order NLO response of a 10,20-diphenyporphyrinato nickel(II) complex carrying a phenyethynyl based push-pull system in the 5- and 15-positions. *J. Porph. Phtal.* **2004**, *8*, 1311-1324.

(10) Pizzotti, M.; Tessore, F.; Orbelli Biroli, A.; Ugo, R.; De Angelis, F.; Fantacci, S.; Sgamellotti, A.; Zuccaccia, D.; Macchioni, A. An EFISH, theoretical, and PGSE NMR investigation on the relevant role of aggregation on the second order NLO response in $CHCl_3$ of the push-pull chromophores [5-[[4'-(Dimethylamino)phenyl]ethynyl]-15-[(4"-nitrophenyl)ethynyl]-10,20-diphenylporphyrinate] M(II) (M = Zn, Ni). *J. Phys. Chem. C* **2009**, *113*, 11131-11141.

(11) Kim, K. S.; Noh, S. B.; Katsuda, T.; Ito, S.; Osuka, A.; Kim, D. Charge transfer induced enhancement of near-IR two-photon absorption of 5,15-bis(azulenylethynyl) zinc(II) porphyrins. *Chem. Commun.* **2007**, 2479-2481.

(12) Collini, E.; Mazzuccato, S.; Zerbetto, M.; Ferrante, C.; Bozio, R.; Pizzotti, M.; Tessore, F.; Ugo, R. Large two photon absorption cross section of asymmetric Zn(II) poprhyrin complexes substituted in the meso or β pyrrolic position by -C≡C-C_6H_4X moieties (X = NMe_2, NO_2). *Chem. Phys. Lett.* **2008**, *,454,* 70-74.

(13) De Angelis, F.; Fantacci, S.; Sgamellotti, A.; Pizzotti, M.; Tessore, F.; Orbelli Biroli, A. Time-dependent and coupled-perturbed DFT and HF investigations on the absorption spectrum and non-linear optical properties of push-pull M(II)-porphyrin complexes (M = Zn, Cu, Ni). *Chem. Phys. Lett.* **2007**, *447*, 10-15.

(14) Li, L. –L.; Diau, E. W. –G. Porphyrin-sensitized solar cells. *Chem. Soc. Rev.* **2013**, *42*, 291-304.

(15) Orbelli Biroli, A.; Tessore, F.; Pizzotti, M.; Biaggi, C.; Ugo, R.; Caramori, S.; Aliprandi, A.; Bignozzi, C. A.; De Angelis, F.; Giorgi, G.; Licandro, E.; Longhi, E. A multitechnique physicochemical investigation of various factors controlling the photoaction spectra and of some aspects of the electron transfer for a series of push-pull Zn(II) porphyrins acting as dyes in DSSCs. *J. Phys. Chem. C* **2011**, *115*, 23170-23182.

(16) Di Carlo, G.; Orbelli Biroli, A.; Pizzotti, M.; Tessore, F.; Trifiletti, V.; Ruffo, R.; Abbotto, A.; Amat, A.; De Angelis, F.; Mussini, P. R. Tetraaryl Zn^{II} porphyrinates substituted in β-pyrrolic positions as sensitizers in dye-sensitized solar cells: a comparison with *meso*-disubstituted push-pull Zn^{II} porphyrinates. *Chem. Eur. J.* **2013**, *19*, 10723-10740.

(17) Levine, B. F.; Bethea, C. G. Molecular hyperpolarizabilities determined from conjugated and nonconjugated organic liquids. *Appl. Phys. Lett.* **1974**, *24*, 445-447.

(18) Singer, K. D.; Garito, A. F. Measurements of molecular second order optical susceptibilities using dc induced second harmonic generation. *J. Chem. Phys.* **1981**, *75*, 3572-3580.

(19) Ledoux, I.; Zyss, J. Influence of the molecular environment in solution measurements of the second-order optical susceptibility for urea and derivatives. *Chem. Phys.* **1982**, *73*, 203-213.

(20) Dale, S. H.; Elsegood, M. R. J. Hydrogen-bonding adducts of benzenepolycarboxylic acids with *N*,*N*-dimethylformamide: benzene-1,4-dicarboxylic acid *N*,*N*-dimethylformamide disolvate,benzene-1,2,4,5-tetracarboxylic acid *N*,*N*-dimethylformamide tetrasolvate and benzene-1,2,3-tricarboxylic acid *N*,*N*-dimethylformamide disolvate monohydrate. *Acta Cryst. C* **2004**, 60 , o444-o448.

(21) Etter, M. C. Encoding and decoding hydrogen-bond patterns of organic compounds. *Acc. Chem. Res.* **1990**, *23*, 120-126.

(22) Bellachioma, G; Ciancaleoni, G.; Zuccaccia, C.; Zuccaccia, D.; Macchioni, A. NMR investigation of non-covalent aggregation of coordination compounds ranging from dimers and ion-pairs up to nano-aggregates. *Coord. Chem. Rev.* **2008**, *252*, 2224-2238.

(23) Pregosin, P. S. Spectroscopic properties of inorganic and organometallic compounds: techniques, materials and applications. Yarwood, J., Douthwaite, R., Duckett, S. Eds.; RSC Publishing, 2011, 42, 248-268.

(24) Avram, L.; Cohen, Y. Diffusion NMR of molecular cages and capsules. *Chem. Soc. Rev.* **2015**, *44*, 586-602.

(25) Rocchigiani, L.; Macchioni, A. Disclosing the multi-faceted world of weakly interacting inorganic systems by means of NMR spectroscopy. *Dalton Trans.* **2016**, *45*, 2785-2790.

(26) Mussini, P. R.; Orbelli Biroli, A.; Tessore, F.; Pizzotti, M.; Biaggi, C.; Di Carlo, G.; Lobello, M. G.; De Angelis, F. Modulating the electronic properties of asymmetric push-pull and symmetric Zn(II)-diarylporphyrinates with *para* substituted phenylethynyl moieties in 5,15 *meso* positions: a combined electrochemical and spectroscopic investigation. *Electrochim. Acta* **2012**, *85*, 509-523.

(27) Pizzotti, M.; Ugo, R.; Annoni, E.; Quici, S.; Ledoux-Rak, I.; Zerbi, G.; Dal Zoppo, M.; Fantucci, P. C.; Invernizzi, I. A critica evaluation of EFISH and THG-non-linear optical

response of asymmetrically substituted *meso*-tetraphenyl porphyrins and their metal complexes. *Inorg. Chim. Acta* **2002**, *340*, 70-80.

(28) Willetts, A.; Rice, J. E.; Burland, D. M.; Shelton, D. P. Problems in the comparison of theoretical and experimental hyperpolarizabilities. *J. Chem. Phys.* **1992**, *97*, 7590-7599.

(29) Tomasi, J.; Mennucci, B.; Cammi, R. Quantum mechanical continuum solvation models. *Chem. Rev.* **2005**, *105*, 2999-3093.

(30) Mennucci, B. Polarizable continuum model. *Wiley Interdiscip. Rev.: Comput. Mol. Sci.* **2012**, *2*, 386-404.

(31) Jacquemin, D.; Planchat, A.; Adamo, C.; Mennucci, B. TD-DFT assessment of functional for 0-0 transition in solvated dyes. *J. Chem. Theory Comput.* **2012**, *8*, 2359-2372.

(32) Suponitsky, K. Y.; Tafur, S.; Masumov, A. E. Applicability of hybrid density functional theory methods to calculation of quadratic hyperpolarizability. *J. Chem. Phys.* **2008**, *129*, 044109-11.

(33) Bale, D. H.; Eichinger, B. E.; Liang, W.; Li, X.; Dalton, L. R.; Robinson, B. H.; Reid, P. J. Dielectric dependence of the first molecular hyperpolarizability for electro-optic chromophores. *J. Phys. Chem. B* **2011**, *115*, 3505-3513.

(34) Johnson, L. E.; Dalton, L. R.; Robinson, B. H. Optimizing calculations of electronic excitations and relative hyperpolarizabilities of electrooptic chromophores. *Acc. Chem. Res.* **2014**, *47*, 3258-3265.

(35) Lu, S.; Chiu, C. –C.; Wang, Y. –F. Density functional theory calculations of dynamic first hyperpolarizabilities for organic molecules in organic solvent: comparison to experiment. *J. Chem. Phys.* **2011**, *135*, 134104-7.

(36) Gaussian 09, Revision **D.01**, Frisch, M. J.; Trucks, G. W.; Schlegel, H. B.; Scuseria, G. E.; Robb, M. A.; Cheeseman, J. R.; Scalmani, G.; Barone, V.; Mennucci, B.; Petersson, G. A.; Nakatsuji, H.; Caricato, M.; Li, X.; Hratchian, H. P.; Izmaylov, A. F.; Bloino, J.; Zheng, G.; Sonnenberg, J. L.; Hada, M.; Ehara, M.; Toyota, K.; Fukuda, R.; Hasegawa, J.; Ishida, M.; Nakajima, T.; Honda, Y.; Kitao, O.; Nakai, H.; Vreven, T.; Montgomery,

J. A., Jr.; Peralta, J. E.; Ogliaro, F.; Bearpark, M.; Heyd, J. J.; Brothers, E.; Kudin, K. N.; Staroverov, V. N.; Kobayashi, R.; Normand, J.; Raghavachari, K.; Rendell, A.; Burant, J. C.; Iyengar, S. S.; Tomasi, J.; Cossi, M.; Rega, N.; Millam, J. M.; Klene, M.; Knox, J. E.; Cross, J. B.; Bakken, V.; Adamo, C.; Jaramillo, J.; Gomperts, R.; Stratmann, R. E.; Yazyev, O.; Austin, A. J.; Cammi, R.; Pomelli, C.; Ochterski, J. W.; Martin, R. L.; Morokuma, K.; Zakrzewski, V. G.; Voth, G. A.; Salvador, P.; Dannenberg, J. J.; Dapprich, S.; Daniels, A. D.; Farkas, Ö.; Foresman, J. B.; Ortiz, J. V.; Cioslowski, J.; Fox, D. J. Gaussian, Inc., Wallingford CT, 2009.

(37) Becke, A. D. Density-functional thermochemistry. III. The role of exact exchange. *J. Chem. Phys.* **1993**, *98*, 5648-5652.

(38) Binkley, J. S.; Pople, J. A.; Hehre, W. J. Self-consistent molecular orbital methods. 21.Small split-valence basis sets for first-row elements. *J. Am. Chem. Soc.* **1980**, *102*, 939-947.

(39) Bergendahl, L. T.; Paterson, M. J. Excited states of porphyrin and porphycene aggregates: computation insights. *Comp. Theor. Chem.* **2014**, *1040-1041*, 274-286.

(40) Tao, J.; Perdew, J. P.; Staroverov, V. N.; Scuseria, G. E. Climbing the density functional ladder: nonempirical meta-generalized gradient approximation designed for molecules and solids. *Phys. Rev. Lett.* **2003**, *91*, 146401-4.

(41) Grimme, S.; Antony, J.; Ehrlich, S.; Krieg, H. J. A consistent and accurate ab initio parametrization of density functional dispersion correction (DFT-D) for the 94 elements H-Pu. *J. Chem. Phys.* **2010**, *132*, 154104-19.

(42) Sousa, S. F.; Fernandes, P. A.; Ramos, M. J. General performance of density functionals. *J. Phys. Chem. A* **2007**, *111*, 10439-10452.

(43) Yang, X.; Hall, M. B. Mechanism of water splitting and oxygen-oxygen bond formation by a mononuclear ruthenium complex. *J. Am. Chem. Soc.* **2010**, *132*, 120-130.

(44) Petrović, P. V.; Janjić, G. V.; Zarić, S. D. Stacking interactions between square-planar metal complexes with 2,2'-bipyridine ligands. Analysis of crystal structures and quantum chemical calculations. *Cryst. Growth Des.* **2014**, *14*, 3880-3889.

(45) Tyrrell, H. J. W.; Harris, K. R. *Diffusion in liquids*; Butterworth: London, 1984.

(46) Mills, R. Self-diffusion in normal and heavy water in the range 1-45.deg. *J. Phys. Chem.* **1973**, *77*, 685-688.

(47) Zuccaccia, D.; Macchioni, A. An accurate methodology to identify the level of aggregation in solution by PGSE NMR measurements: the case of half-sandwich diamino ruthenium(II) salts. *Organometallics* **2005**, *24*, 3476-3486.

(48) Yeo, H.; Austin, D. J.; Li, L.; Cheng, Y. -C. Novel antiviral helioxanthin analogs. PCT/US2005/014698.

(49) Gouterman, M. Spectra of porphyrins. *J. Mol. Spectrosc.* **1961**, *6*, 138-163.

(50) Nappa, M.; Valentine, J. S. The influence of axial ligands on metalloporphyrin visible absorption spectra. Complexes of tetraphenylporphyrnatozinc. *J. Am. Chem. Soc.* **1978**, *100*, 5075-5080.

(51) Ray, P. C.; Leszczynski, J. Nonlinear optical properties of highly conjugated push-pull porphyrin aggregates: the role of intermolecular interaction. *Chem. Phys. Lett.* **2006**, *419*, 578-583.

(52) Takei, K.; Takahashi, R.; Noguchi, T. Correlation between the hydrogen-bond structures and the C=O stretching frequencies of carboxylic acids as studied by density functional theory calculations: theoretical basis for the interpretation of infrared bands of carboxylic groups in proteins. *J. Phys. Chem. B* **2008**, *112*, 6725-6731.

(53) Annoni, E.; Pizzotti, M.; Ugo, R.; Quici, S.; Morotti, T.; Casati, N.; Macchi, P. The effect on *E*-stilbazoles second order NLO response by axial interaction with M(II) 5,10,15,20-tetraphenyl porphyrinates (M = Zn, Ru, Os): a new cristalline packing with very large holes. *Inorg. Chim. Acta* **2006**, *359*, 3029-3041.

(54) Huyskens, F. L.; Huyskens, P. L.; Persoons, A. P. Solvent dependence of the first hyperpolarizability of *p*-nitroanilines: difference between nonspecific dipole-dipole interactions and solute-solvent H-bonds. *J. Chem. Phys.* **1998**, *108*, 8161-8171.

(55) Huyskens, F. L.; Huyskens, P. L.; Persoons, A. P. Influence of solvent-solute H-bonds of *p*-nitroanilines on the hyper-Rayleigh scattering in solutions. Preferential environment for non-linear optically active molecules in binary solvent mixtures. *J. Mol. Struct.* **1998**, *448*, 161-170.

(56) Bartkowiak, W.; Lipkowski, P. Hydrogen-bond effects on the electronic absorption spectrum and evaluation of nonlinear optical properties of an aminobenzofuranone derivative that exhibits the largest positive solvatochromism. *J. Mol. Mod.* **2005**, *11*, 317-322 and references therein.

(57) Riley, K. E.; Merz, K. M. Insights into the strength and origin of halogen bonding: the halobenzene-formaldehyde dimer. *J. Phys. Chem. A* **2007**, *111*,1688-1694.

(58) Cariati, E.; Forni, A.; Biella, A.; Metrangolo, P.; Meyer, F.; Resnati, G.; Righetto, S.; Tordin, E.; Ugo, R. Tuning second-order NLo response through halogen bonding. *Chem. Commun.* **2007**, 2590-2592.

(59) Macchioni, A.; Ciancaleoni, G.; Zuccaccia, C.; Zuccaccia, D. Determining accurate molecular sizes in solution through NMR diffusion spectroscopy. *Chem. Soc. Rev.* **2008**, *37*, 479-489.

(60) Rocchigiani, L.; Bellachioma, G.; Ciancaleoni, G.; Crocchianti, S.; Laganà, A.; Zuccaccia, C.; Zuccaccia, D.; Macchioni, A. Anion-dependent tendency of di-long-chain quaternary ammonium salts to form ion quadruples and higher aggregates in benzene. *ChemPhysChem* **2010**, *11*, 3243-3254.

(61) Würthner, F.; Yao, S.; Debaerdemaeker, T.; Wortmann, R. Dimerization of merocyanine dyes. Structural and energetic characterization of dipolar dye aggregates and implications for nonlinear optical materials. *J. Am. Chem. Soc.* **2002**, *124*, 9431-9447.

(62) Kang, H.; Facchetti, A.; Jiang, H.; Cariati, E.; Righetto, S.; Ugo, R.; Zuccaccia, C.; Macchioni, A.; Stern, C.; Liu, Z.; Ho, S. –T.; Brown, E. C.; Ratner, M. A.; Marks, T. J. Ultralarge hyperpolarizability twisted π-electronsystem electro-optic chromophores: synthesis, solid-state and solution-phase structural characteristics, electronic structures, linear and nonlinear optical properties, and computational studies. *J. Am. Chem. Soc.* **2007**, *129*, 3267-3286.

(63) Tessore, F.; Locatelli, D.; Righetto, S.; Roberto, D.; Ugo, R.; Mussini, P. An investigation on the role of the nature of sulfonated ancillary ligands on the strength and concentration dependence of the second-order NLO responses in $CHCl_3$ of Zn(II) complexes with 4,4'-*trans*-$NC_5H_4CH{=}CHC_6H_4NMe_2$ and 4,4'-*trans,trans*-$NC_5H_4(CH{=}CH)_2C_6H_4NMe_2$. *Inorg. Chem.* **2005**, *44*, 2437-2442.

For Table of Contents only

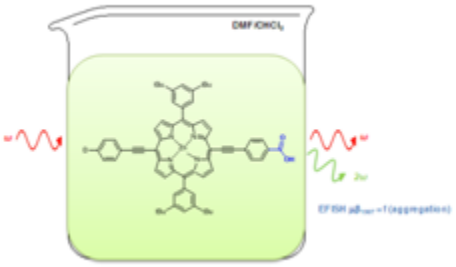

The presence of a –COOH acceptor group in push-pull Zn^{II} porphyrinates strongly affects their EFISH $\mu\beta_{1907}$ response in $CHCl_3$ and DMF solution by aggregation.